Bone Geometry, Density, and Microarchitecture in the Distal Radius and Tibia in Adults With Marfan Syndrome Assessed by HR-pQCT

Folkestad, Lars; Groth, Kristian A.; Shanbhogue, Vikram; Hove, Hanne; Kyhl, Kasper; Østergaard, John R.; Jørgensen, Niklas Rye; Andersen, Niels H.; Gravholt, Claus H.

Published in:
Journal of Bone and Mineral Research

DOI (link to publication from Publisher):
10.1002/jbmr.4138

Publication date:
2020

Document Version
Accepted author manuscript, peer reviewed version

HOLOGIC®
The Science of Sure

Powerful images.
Clear answers.

Manage Patient's concerns about Atypical Femur Fracture*

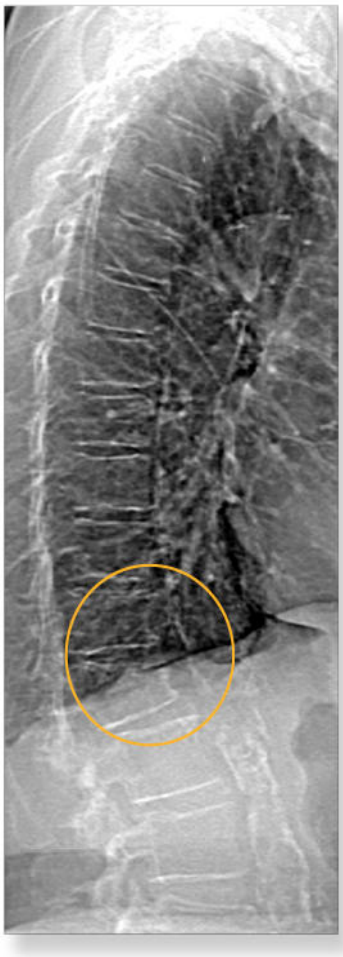

Vertebral Fracture Assessment – a critical part of a complete fracture risk assessment

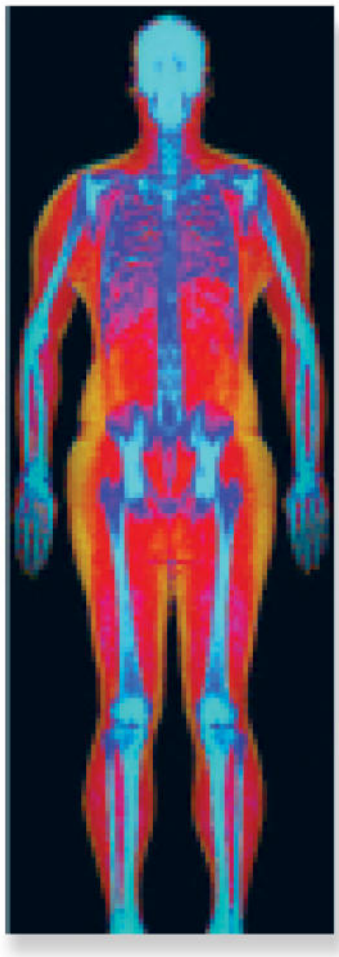

Advanced Body Composition® Assessment – the power to see what's inside

Contact your Hologic rep today at BSHSalesSupportUS@hologic.com

*Incomplete Atypical Femur Fractures imaged with a Hologic densitometer, courtesy of Prof. Cheung, University of Toronto

www.hologic.com | dxaperformance.com | 1.800.442.9892

Bone Geometry, Density, and Microarchitecture in the Distal Radius and Tibia in Adults With Marfan Syndrome Assessed HR-pQCT

Lars Folkestad[1,2], Kristian A. Groth[3], Vikram Shanbhogue[1], Hanne Hove[4,5], Kasper Kyhl[6], John R. Østergaard[7], Niklas Rye Jørgensen[8,9] Niels H. Andersen[10] and Claus H. Gravholt[3,11]

1) Department of Endocrinology and Metabolism, Odense University hospital, Denmark
2) Department of Clinical Research, University of Southern Denmark, Denmark
3) Department of Cardiology, Aarhus University Hospital, 8200 Aarhus N, Denmark
4) Department of Pediatrics , Copenhagen University, Hospital, Rigshospitalet, 2100 Copenhagen, Denmark
5) The RAREDIS Database, Section of Rare Diseases, Department of Clinical Genetics and Pediatrics, Copenhagen University Hospital, Rigshospitalet, 2100 Copenhagen, Denmark
6) Department of Cardiology, Rigshospitalet, 2100 Copenhagen, Denmark
7) Centre for Rare Diseases, Department of Pediatrics, Aarhus University Hospital, 8200 Aarhus N, Denmark
8) Department of Clinical Biochemistry, Rigshospitalet, Copenhagen, Denmark
9) Department of Clinical Medicine, Faculty of Health and Medical Sciences, University of Copenhagen, 2100 Copenhagen, Denmark
10) Department of Cardiology, Aalborg University Hospital, 9100 Aalborg, Denmark
11) Department of Endocrinology, Aarhus University Hospital, 8200 Aarhus, Denmark

*) Corresponding author: Lars Folkestad, MD, PhD, Department of Endocrinology and Metabolism, Odense Universityhospital, Sdr Boulevard 29, Osteoporose klinikken, 5000 Odense C. E-Mail: LFolkestad@health.sdu.dk
ORCID: 0000-0001-6266-6439

Wordcount: 3538
Tables: 4
Figures: 3

This article has been accepted for publication and undergone full peer review but has not been through the copyediting, typesetting, pagination and proofreading process which may lead to differences between this version and the Version of Record. Please cite this article as doi: 10.1002/jbmr.4138

ABSTRACT:
Marfan Syndrom (MFS) is a hereditary disorder of connective tissue caused by mutations in the fibrillin-1 gene. Studies have shown that patients with MFS have lower bonemass but little is known about the other constituents of bone strength. We hypothesize that patients with MFS will have larger bone area and compromised cortical microarchitecture in comparison to non-MFS individuals. A total of 74 adult patients with MFS and 145 age and gender matched non-MFS reference individuals (ref.gr) were included in this study. High-resolution peripheral quantitative computed tomography (HR-pQCT) at the distal radius and distal tibia and dual-energy X-ray absorptiometry of total hip and the lumbar spine were performed, and bone turn-over and sex hormones were measured. Patients with MFS had significantly lower areal bone mineral density (BMD) at the total spine (-13%) and total hip (-7%) when compared with the ref.gr. Patients with MFS had significantly larger total bone area at both the radius (+27%) and tibia (+34%). Volumetric BMD at both the measured sites showed significantly reduced total, trabecular and cortical volumetric BMD in patients with MFS compared to the ref.gr. The microarchitectural parameters at the radius and tibia were compromised in patients with MFS with significantly reduced trabecular number and thickness leading to a higher trabecular separation and significantly reduced cortical thickness and increased cortical porosity compared to the reference group. The differences in bone-density, -geometry or -microarchitecture was not explained by increased bone turnover markers or circulating levels of sex hormones. We conclude patients with MFS had altered bone geometry, altered bone microstructure and lower bone mass (lower aBMD and vBMD at all sites) compared to healthy reference individuals. Future studies should focus on fracture rates and fracture risk in adult and aging patients with MFS.

Keywords:
Marfan Syndrom; Inherited disorders; trabecular bone; osteoporosis; fracture risk; tgf-beta

Introduction

Marfan Syndrome (MFS) is an hereditary connective tissue disorder with variable expressivity and musculoskeletal, cardiac and ocular abnormalities in addition to manifestations involving lung, skin and central nervous system [1,2]. The annual median incidence of MFS was 0.19/100.000 (range 0.0-0.7) from 1977 to 2015 and the prevalence is 6.5 per 100.000 in Denmark [3]. MFS is commonly caused by mutations in the fibrillin-1 gene (FBN1) located on chromosome 15 causing altered elastin synthesis, while 27% are de novo mutations [1,4,5]. Patients with MFS have an increased all-cause mortality hazard ratio for both men and women compared to the general population, related to their increased risk of death due to cardiovascular and respiratory diseases [6]. Furthermore, musculoskeletal conditions such as osteoporosis, craniofacial manifestations and myopathy are frequent co-morbid features in MFS [2]. Several bone mineral density (BMD) studies using dual energy x-ray absorptiometry (DXA) have demonstrated reduced BMD in children [7,8] and adults [9–12] with MFS compared to reference groups. In a longitudinal study of children (median age of 11.9 years) with MFS, the bone mass at the axial and appendicular levels worsened from childhood to adulthood, and was related to lower muscle mass in the MFS patients [7]. It has been suggested that patients with MFS due to a lower peak bone mass have a higher prevalence of low bone mass in adult life, resulting in increased risk of fractures throughout life. In a recent study of children with MFS, the authors reported an fracture incidence of 29.2/1000 patients with MFS (aged 3-16) compared to 15.8/1000 in an matched reference group [8]. There are currently no data on fracture risk in adult patients with MFS, and no studies have been able to look at any differences in fracture risk between the sexes.

Fibrillin-1 in microfibrils interact with the large latent complex consistent of TGF-β (transforming growth factor beta), two precursor peptides and LTBP-1 (latent TGF-β-binding protein 1) [7,13]. The loss of fibrillin-1 protein, as caused by the FBN1 mutations in MFS, affects the pool of TGF-β. In mice, TGF-β has been shown to positively regulate osteoblast proliferation and differentiation [7,13]. Furthermore, fibrillin-1 is a structural component of the bone marrow niche, that supports self-renewal of mesenchymal stem cells, lineages determination and progenitor cells [4]. Fibrillin-1 deficiency may commit the mesenchymal stem cells towards adipogenesis rather than towards an osteoblastic lineage, as suggested by progressive bone loss in MFS mice [4].

DXA based assessment of BMD is a 2-dimensional condensation of a 3-dimensional structure and does not differentiate whether the variation in BMD arises from differences in cortical mass, trabecular mass or external bone size. High resolution peripheral quantitative computed tomography scanner (HR-pQCT) enables assessment of trabecular and cortical bone microarchitecture and volumetric bone mineral density (vBMD) at the distal radius and distal tibia with a spatial resolution of 82 µm. The ability of HR-pQCT to resolve the trabecular and cortical microarchitecture lends itself to estimating the biomechanical properties of the radius and tibia by voxel-based linear finite element analysis, whereby estimated failure load can be calculated.

There are currently limited data on bone compartment specific vBMD and bone microarchitecture in adult patients with MFS. The aim of this study was to evaluate bone geometry, microstructure and estimated bone strength in adult Danish patients with MFS compared to healthy non-MFS matched reference individuals using HR-pQCT. Based on earlier DXA studies and conventional

wisdom that MFS patients have larger bone size, we hypothesize that patients with MFS will have larger bone area and compromised cortical microarchitecture in comparison to reference individuals. Furthermore we hypothesize that the differences will be accentuated by age and postmenopausal status.

Methods and participants:

We invited all known patients with MFS older than 18 years of age from the outpatient clinic at the Department of Cardiology, Aarhus University Hospital or Center of Rare Diseases, Rigshospitalet. 230 eligible patients were invited to participate in the study by mail and informed about the study at routine clinical visits. Patients could not participate if they were pregnant, had other metabolic bone diseases (e.g Pagets disease, multiple myeloma, osteogenesis imperfecta or primary hyperparathyroidism), or if they were treated with drugs that alter bone metabolism (e.g. steroids, anti-estrogen treatment, strontiumranelate, PTH-analogues, denosumab or bisphosphonates). Recruitment was started in late 2012 and ended in late 2015.

Moura et al. [(11)], found a 17% lower areal BMD in the hip in patients with MFS compared with healthy controls. We anticipated that the same difference would be present when evaluating bone volume to tissue volume ratio in the radius, as this parameter is best correlated to areal BMD. Hansen et al. [(14)] found in healthy Danes a bone volume to tissue volume ratio (BV/TV) of 0.14±0.03. Anticipating a 17% difference in BV/TV between the two groups with an alpha of 0.05 and beta of 0.2 we aimed to include 30 males age 18-80 years, 30 premenopausal women and 30 postmenopausal women.

Each MFS patient was matched by age (±5years), menopausal state (yes/no) and gender to two individuals where possible (n=145) from the cohort of 499 healthy adult women and men participating in a separate study aimed at establishing HR-pQCT reference data in the adult Danish population as described by Hansen et al. [14].

Using self-administered questionnaires we assessed pharmacological treatment and menopausal status (more than 1 year since last menstruation). Body weight and height were measured using a Seca model 708 scale (Seca, Hamburg, Germany) and a wall-mounted Harpeden stadiometer (Holtain, Crymych, UK), respectively. All participants provided informed consent, and the local ethics review board approved the study (no. 20090069, no. 20090131, no. 20100023, no. 20120135).

High Resolution Peripheral Quantitative Computed Tomography

We scanned the non-dominant distal radius and distal tibia, or in case of a previous fracture at the desired site, the dominant limb, using a HR-pQCT system (Xtreme CT, Scanco Medical AG, Brüttisellen, Switzerland). The manufacturer's standard protocol for patient in vivo scanning was applied, providing a 9.02mm 3D representation of the distal radius and tibia in the axial direction. We used a fixed offset from the bone endplate to the scan region of 9.5 mm in radius and 22.5 mm in tibia. Each image comprised of 110 slices with an isotropic voxel size of 82 µm. The operator viewed the most distal slice for motion artifacts and a maximum of three scans per anatomical site were performed. Image quality was graded after image reconstruction by one of the authors (VS)

using a 5-step scale as suggested by the manufacturer (1 = best; 5 = worst) and images graded 4 or 5 were disregarded. Total vBMD, cortical vBMD (Ct.vBMD), and trabecular vBMD were derived from their respective volumes, calibrated using a scan phantom, and expressed in mg/cm^3. Cortical thickness (Ct.Th, mm) was measured directly as the periosteal-endosteal distance using a distance transformation method, and cortical porosity (Ct.Po, %) was measured as void cortical volume divided by total cortical volume [15,16]. Trabecular number (Tb.N, 1/mm) was measured directly using a distance transformation method based on identification of the trabecular mid-axis [17]. Trabecular thickness (Tb.Th, mm) was derived from Tb.N and trabecular bone volume fraction (BV/TV) as Tb.Th = (BV/TV)/Tb.N, and trabecular separation (Tb.Sp) as (1–[BV/TV])/Tb.N, where BV/TV was derived from Tb.vBMD, assuming a mineral density of fully mineralized bone of 1200 mg/cm^3. Finally, a micro-finite element analysis (FEA) solver using software provided by the manufacturer (Finite Element Analysis Software v1.15; Scanco Medical) was used to estimate failure load in compression, wherein all bone materials were given a Young modulus of 10 GPa and a Poisson ratio of 0.3. From the models, an estimate of failure load in compression was calculated based on the assumption that bone failure occurs when >2% of the elements are strained beyond 0.7% [18]. The coefficient of variation (CV) for geometry, vBMD, microarchitecture, and estimated strength indices ranged from 0.4% to 7.2% in our unit [14].

Dual energy X-ray absorptiometry

Areal BMD (aBMD) of the nondominant hip (total hip region) and the lumbar spine (L_1–L_4) were measured using DXA (Discovery; Hologic, Inc., Waltham, MA, USA). The CV in our unit for measurements of both the hip and spine is 1.5% [19]. Total spine areal BMD was available from 70

of the patients with MFS and all of the reference group. Total aBMD was not calculated in the 4 patients with spinal fusion osteo-synthetic material of the lumbar spine. Total hip areal BMD was available from 72 of the MFS patients and 144 of the reference individuals. Total hip aBMD was not calculated if the participant had had hip replacement surgery.

Biochemical tests

In patients and reference individuals blood samples were drawn between 8 and 10 am after an overnight fast. Blood samples were stored at -80^{o} Celsius until analyses. All analyses were batch analyzed at the same lab for each sub group.

Samples for the bone resorption marker carboxyterminal cross-linked telopeptide of type 1 collagen (CTX) were measured using IDS-iSYS CTX-I (CrossLaps®) assay (Immunodiagnostic Systems, plc, Tyne and Ware, UK) with coefficient of variation of 5.3%, 3.4% and 3.5% at levels of 213, 869 and 2113 ng/L. The bone formation marker N-terminal propeptide of type 1 procollagen (P1NP) was measured using the IDS-iSYS intact P1NP assay (Immunodiagnostic Systems) with CVs of 5.4%, 6.5% and 6.1% at levels of 18.96, 48.48, and 122.10µg/L. The analysis was done in two batches, one for the MFS group and one for the reference group.

Follicle stimulating hormone (FSH), luteinizing hormone (LH), and sex hormone binding globulin (SHBG) were quantitatively determined by immunoassay employing the Cobas e601 electrochemiluminescence measuring unit (Cobas, Roche Diagnostics Limited, Rotkreuz, Switzerland). Testosterone and 17β-estradiol were measured by liquid chromatography tandem

mass spectrometry. The limit of detection was 0.1 nmol/L, and the working range was 0.2–100 nmol/L with a coefficient of variation of <10%.

Statistical analysis

Data are presented as mean ± SD, median [interquartile range] or total number (and per cent) as appropriate. We assessed the distribution of each parameter via normality plots and Shapiro-Wilks W test and compared the two groups using Wilcoxon ranked sum test, students *t*-test, or chi-squared test as appropriate. Values of *p* were two-sided, and the statistical significance level was set at 0.05. To identify the parameters that best distinguish patients with MFS from the reference group, we performed logistic regression analyses using a dummy variable (MFS yes/no) as the dependent variable and the measured HR-pQCT parameters as predictor variables. Pearson's goodness-of-fit and the Akaike information criterion (AIC) were then calculated. The model with the best fit and lowest AIC was selected as identifying the variable that best distinguished the MFS and reference groups. Gender-based differences were assessed by evaluating the parameters that best distinguished the MFS and reference groups in subgroup analysis only including men, women or post-menopausal women. Using the Bonferroni correction by dividing the alpha of 0.05 with the number of variables for bone-mass, -geometry, -microarchitecture and estimated bone strength in our primary analysis (comparing al MFS participants to the reference individuals, number of group comparisons = 26), we obtain a significance level of 0.0019. Lastly we performed a sensitivity analysis excluding patients with MFS diagnosed with osteoporosis (defined as a aBMD t-score of <-2.5 compared to a relevant reference material at either the total spine or total hip sites) from the between group comparison of the HR-pQCT parameters that best distinguished the MFS and

reference groups. All analyses were done based on assessment of pre-study planed primary parameters, and using Stata Statistical Software Release 16.0 (StataCorp LP, College Station, TX, USA).

Results

Basic characteristics

We included 74 Caucasian (42 women) patients with MFS and 145 (82 women) reference individuals. The MFS group were significantly taller compared to the reference group. There were no significant differences in weight, leaving the BMI significantly lower in the MFS group compared to the reference group (Table 1).

Dual energy X-ray absorptiometry

Patients with MFS had significantly lower aBMD at the total spine (0.930±0.15 vs 1.00±0.13 gHA/cm^2, p=0.003) and total hip (0.846±0.13 vs 0.969±0.13 gHA/cm^2, p<0.001) compared to the reference group (Figure 1). Thirteen patients with MFS (mostly postmenopausal women and older men aged more than 50 years of age – individual level data not shown) were diagnosed with osteoporosis.

High Resolution Peripheral Quantitative Computed Tomography

Due to low quality of the scans, we removed 11 radial scans from the MFS group and three radial and five tibial scans from the reference group were excluded. Patients with MFS had significantly larger total bone area reflected in larger trabecular area compared to the reference group at both the

radius and tibia. Cortical area on the other hand was significantly smaller in the MFS group compared to the reference group at both these sites (Table 2 and 3). Furthermore, total, trabecular and cortical vBMD was reduced at both the measured sites vBMD in patients with MFS compared to the reference group. Similarly, the microarchitectural parameters at the radius and tibia were compromised in patients with MFS with significantly reduced trabecular number (Tb.N) and trabecular thickness (Tb.Th) leading to a higher trabecular separation (Tb.Sp) and significantly reduced cortical thickness (Ct.Th) and increased cortical porosity (Ct.Po) compared to the reference group. While there was a tendency towards reduced estimated failure load at the radius, it was significantly reduced at the tibia in the MFS group compared to the reference group.

Bone-microarchitecture, bone-geometry and volumetric bone mineral density parameters that best distinguish MFS patients from the reference group

Results of the logistic regression modelling (Table 3) showed that Ct.Po was the best parameter to distinguish between patients with MFS and the reference group overall, and was also the best microarchitecture parameter in this regard. While trabecular area was the best geometrical parameter and total vBMD was the best densitometric parameter, Tb.N was the best trabecular microarchitecture parameter (Figure 2 and 3).

Subgroup analysis by sex and menopausal state.

Height, weight and the best HR-pQCT between group determinants have been summarized in Supplement 1 (table S1-S3).

Changes in bone geometry, density, microarchitecture and strength over time

As illustrated by Figure 2 and Figure 3 the between group differences were greater for some of the variables with increasing age in the radius and the tibia. Cortical porosity seemed to increase more in the MFS group with increasing age than in the reference group. The trabecular area and trabecular number seemed to be relative stable with increasing age. Total vBMD seemed to be lower with age and to a larger extent in the MFS group compared to the reference group. The estimated failure load decreases with increasing age, but follows the same rate of change in the MFS group and the reference group.

Bone turnover markers

All of the MFS group and 120 of the reference group had bone turnover markers (BMT) measured and analyzed. While bone resorption was equal in the two groups, bone formation was higher in the MFS group (Table 4).

Gonadotrophins and sex-steroids

All of the MFS group and 110 of the reference group had gonadotrophins, SHBG, testosterone and 17β-estradiol measured. There were no differences in gonadotropins comparing MFS to the reference group. Men with MFS had higher 17β-estradiol levels and premenopausal women with MFS had lower levels of testosterone compared to their control groups (Table 4).

Sensitivity analysis

After excluding patients with osteoporosis from the MFS group, the differences in failure load, cortical porosity, trabecular number, trabecular area and total volumetric BMD did not change significantly for radius or tibia except tibial failure load (data not shown).

Multiple testing

In our main analysis we found 25 parameters to be significantly different between the two groups, and 23 of these had a significance level below the Bonferroni correction alpha of 0.0019. Only failure load in tibia could not be regarded as significantly lower in the MFS group after Bonferroni correction.

Discussion

This is the first study assessing bone structural parameters and bone biomechanics using HR-pQCT in a large adult population of patients with MFS. Patients with MFS had lower overall and compartment specific volumetric densities and deficits in microarchitectural parameters with fewer and thinner trabeculae leading to a higher trabecular separation, and thinner, more porous cortices in the distal tibia and radius, compared to a reference group randomly selected individuals from the general population. However, the negative impact of the reduced density and compromised structural integrity was compensated by the overall increase in bone size resulting in patients with MFS having similar estimated bone strength in comparison to the reference group.

In our study, we found lower aBMD and vBMD in patients with MFS compared to the reference group. Several authors have observed a reduced aBMD at the appendicular and axial skeleton in

patients with MFS [8–12]. Studies in children with MFS have shown lower aBMD in comparison to their healthy counterparts indicating that patients with MFS will have a lower peak bone mass that may influence the risk of osteoporosis in later life [8,13,20,21]. We found that both men and women had lower aBMD of the hip and spine as well as reduced vBMD of both radius and tibia when compared to their reference groups (Supplementary data). In a large French study by Moura et al [11] including 130 adults with MFS with a mean age of 34.7±10.7 years, the authors found that both women and men had lower aBMD z-scores at both the hip and the wrist [11] consistent with our findings at both the radius and total hip.

There is a paucity of data on bone-microarchitecture assessed invasively or non-invasively using imaging modalities in patients with MFS. In a systematic review and meta-analysis including 40 studies using HR-pQCT and evaluating fracture risk, Mikolajewicz N et.al. [22] reported that total vBMD, trabecular vBMD as well as cortical vBMD and cortical thickness were reliable predictors of fractures. Furthermore, Hansen S et al [23] found that trabecular number and spacing, cortical thickness and cortical area correlates moderately to very highly with the maximum compressive strength of the hip [23]. All of these parameters were found to be negatively affected in the MFS patients in our study, indicating a higher fracture risk in patients with MFS. No population-based studies on fracture rates or fracture risk is currently available in adult patients with MFS. However, children with MFS have an almost twice as high fracture incidence as compared to non MFS children [24].

Despite finding large differences in both the trabecular and the cortical compartments in patients with MFS, estimated bone strength was not significantly different from the reference group after controlling for multiple testing. Whole bone strength and the ability of bone to resist fracture depends not only on the amount of bone mass and bone microarchitecture, but also on the spatial distribution of this mass and structure [25] . The most efficient adaptation to compromises in bone mass or bone microarchitecture is to distribute the bone material further from the center of the bone, thereby improving bone resistance [26]. Consistent with this hypothesis, are findings of a larger total and trabecular bone area could represent an adaptive process resulting in preserved estimates of bone strength.

The $Fbn1^{mgR/mgR}$ mouse model, harbor mutations in the FBN1 and display a progressive form of MFS [27]. In a study comparing $Fbn1^{mgR/mgR}$ mice to wild type using μCT, the MFS mice had 15% reduced BV/TV, 19.7% reduced vBMD and lower trabecular thickness, and larger trabecular separation [28]. This finding is similar to our HR-pQCT findings in both the radius and the tibia. Contrary to our findings of elevated P1NP but not CTX, the MFS mice had increased bone resorption, but normal bone formation [28].

Hypogonadism in both men and women is a risk factor for osteoporotic fractures [29]. Accelerated bone loss and altered bone structure and geometry can be caused by hypogonadism. However, hypogonadism does not seem to be caused of the differences we found in the MFS population, although discrete differences were observed with significantly increased 17β-estradiol in males with MFS and lower testosterone among premenopausal women.

This is not a longitudinal study, but if patients with MFS suffered accentuated bone loss with increasing age, the differences between the two groups in our study would be larger in the oldest age groups. This was not the case for most of the parameters that best differentiated between the MFS and the reference group. However, the inter-group differences in cortical porosity seemed to increase with increasing age. Cortical thinning and increased cortical porosity happens with increasing age in healthy aging humans [30]. Cortical porosity is caused by intracortical remodeling, and increases bone fragility exponentially [31,32], and 70% of all bone-loss with increasing age is cortical bone loss [32]. This could influence the choice of fracture prevention drugs to treat patients with MFS if they develop osteoporosis. In a HR-pQCT study including 247 postmenopausal women aged 61±5 years comparing denosumab and alendronate, denosumab reduced remodeling more rapidly and decreased porosity more than alendronate [32,33]. There is no evidence on the prevention or treatment of osteopenia or osteoporosis in MFS, and general guidelines should be followed at the current time [2].

We found increased Ct.Po in patients with MFS. We know from other diseases of collagen deficiencies, such as Osteogenesis Imperfecta, that in such conditions increased Ct.Po is frequent [34]. Even though we could not show increased bone-turnover markers in our study, we cannot rule out that patients with MFS have periods in life with increased bone remodeling that may lead to increased Ct.Po.

A limitation to our study is that we did not reach our pre-study sample size. Regardless we found large differences between the three groups even in our sub-group analysis. Another potential limitation of our study was the application of the HR-pQCT standard patient protocol for image acquisition, which entails a fixed offset from the extremity endplate. The measurement site would thus vary with differing lengths of the radius and tibia, being relatively more distally located in taller subjects, leading to a relative over- and underrepresentation of trabecular and cortical bone, respectively [35]. Patients with MFS were significantly taller than the reference group and the differences noted in the cortical compartment, could in part, be explained by the relatively more distal metaphyseal scan location in patients with MFS. However as observed in the study by Shanbhogue et al. [36], while there was a significant morphological variation in Ct.Th using a relative limb length scan region instead of a fixed offset scan region, the Ct.Po was not significantly affected at the radius. A further limitation to the HR-pQCT system is that the Tb.Sp and Tb.Th are not directly measured, but are derived from the measures of trabecular vBMD and Tb.N. Therefore, the differences in Tb.Sp and Tb.Th should be treated with some caution. Finally, FEA results which only reflect impacts of bone geometry and microarchitecture on bone strength should be interpreted with caution since the FEA solver used in this study assumes fixed, homogeneous material properties which are likely not true for patients with MFS. Our findings of deficits in the trabecular and cortical compartments was consistent across both the radius and tibia in the patients with MFS and we argue that patients with MFS do indeed have altered bone-mass, -geometry and both cortical and trabecular -microarchitecture.

The study does have several strengths, firstly we included a large group of patients with MFS with a wide age span and a reference group of otherwise healthy and randomly selected reference individuals. Secondly, we recruited participants with genetic and clinically verified diagnosis of MFS identified through the National Patient Register [3] and verified by individual chart review according to the Ghent criteria [37]. Lastly, the participants were recruited nationwide, thus limiting the risk of selection bias.

Conclusion

In conclusion, patients with MFS had deficits in bone mass reflected in lower aBMD and vBMD and compromised trabecular and cortical bone microstructure with fewer, thinner more higher trabecular separation and thinner and more porous cortex at the appendicular skeleton compared to healthy controls. It is likely that the underlying mutations in the FBN1 gene explains these changes. However, these densitometric and microarchitectural alterations did not translate into lower estimated bone strength probably because of the geometrical alterations with larger total and trabecular bone area in patients with MFS. Further studies are necessary to elucidate fracture rates and fracture risk in adult and aging patients with MFS compared to the general population.

Acknowledgments

The authors thank Jane Nielsen and Jeannette Foged Lindegaard for her help in coordinating the study and to all the bio-analytic staff in obtaining consent from the participants and performing the bone scans. Claus H. Gravholt is a member of the European Reference Network on Rare Endocrine Conditions (ENDO-ERN), Project ID number 739543.

Authors roles

Study design: CHA, NHA, KAG, LF; Patient Recruitment: KAG, NHA, JRØ, HH, CHA; Study conduct: LF, VS; Laboratory analysis: NRJ, CHA; Data Analysis; LF, CHA; Drafting manuscript: LF; Revising manuscript and final approval: LF, KAG, VS, HH, KK, JRØ, NRJ, NHA, CHA. LF accepts responsibility for the integrity of the data analysis.

Funding

This study is supported by Department of Clinical Medicine, Aarhus University Hospital and Aarhus University, the Novo Nordisk Foundation (NNF13OC0003234, NNF15OC0016474) and the Familien Hede Nielsen foundation. The funders had no role in study design, data collection and analysis, decision to publish, or preparation of the manuscript.

Bibliography

1. Dean JCS. Marfan syndrome: clinical diagnosis and management. European Journal of Human Genetics. 2007 Jul;15(7):724–33.
2. von Kodolitsch Y, Demolder A, Girdauskas E, Kaemmerer H, Kornhuber K, Muino Mosquera L, Morris S, Neptune E, Pyeritz R, Rand-Hendriksen S, Rahman A, Riise N, Robert L, Staufenbiel I, Szöcs K, Vanem TT, Linke SJ, Vogler M, Yetman A, De Backer J. Features of Marfan syndrome not listed in the Ghent nosology – the dark side of the disease. Expert Review of Cardiovascular Therapy. 2019 Dec 2;17(12):883–915.
3. Groth KA, Hove H, Kyhl K, Folkestad L, Gaustadnes M, Vejlstrup N, Stochholm K, Østergaard JR, Andersen NH, Gravholt CH. Prevalence, incidence, and age at diagnosis in Marfan Syndrome. Orphanet Journal of Rare Diseases [Internet]. 2015 Dec [cited 2019 Oct 28];10(1). Available from: http://www.ojrd.com/content/10/1/153
4. Ramirez F, Caescu C, Wondimu E, Galatioto J. Marfan syndrome; A connective tissue disease at the crossroads of mechanotransduction, TGFβ signaling and cell stemness. Matrix Biology. 2018 Oct;71–72:82–9.
5. Ramirez F, Dietz HC. Marfan syndrome: from molecular pathogenesis to clinical treatment. Current Opinion in Genetics & Development. 2007 Jun;17(3):252–8.
6. Groth KA, Stochholm K, Hove H, Andersen NH, Gravholt CH. Causes of Mortality in the Marfan Syndrome(from a Nationwide Register Study). The American Journal of Cardiology. 2018 Oct 1;122(7):1231–5.
7. Haine E, Salles J-P, Khau Van Kien P, Conte-Auriol F, Gennero I, Plancke A, Julia S, Dulac Y, Tauber M, Edouard T. Muscle and Bone Impairment in Children With Marfan Syndrome: Correlation With Age and *FBN1* Genotype: MUSCLE AND BONE IMPAIRMENT IN MARFAN SYNDROME. Journal of Bone and Mineral Research. 2015 Aug;30(8):1369–76.
8. Trifirò G, Marelli S, Viecca M, Mora S, Pini A. Areal bone mineral density in children and adolescents with Marfan syndrome: Evidence of an evolving problem. Bone. 2015 Apr;73:176–80.
9. Carter N. Bone mineral density in adults with Marfan syndrome. Rheumatology. 2000 Mar 1;39(3):307–9.
10. Le Parc JM, Plantin P, Jondeau G, Goldschild M, Albert M, Boileau C. Bone Mineral Density in Sixty Adult Patients with Marfan Syndrome. Osteoporosis International. 1999 Nov 1;10(6):475–9.
11. Moura B, Tubach F, Sulpice M, Boileau C, Jondeau G, Muti C, Chevallier B, Ounnoughene Y, Le Parc J-M. Bone mineral density in Marfan syndrome. A large case-control study. Joint Bone Spine. 2006 Dec;73(6):733–5.
12. Tobias JH, Dalzell N, Child AH. ASSESSMENT OF BONE MINERAL DENSITY IN WOMEN WITH MARFAN SYNDROME. Rheumatology. 1995;34(6):516–9.
13. Grover M, Brunetti-Pierri N, Belmont J, Phan K, Tran A, Shypailo RJ, Ellis KJ, Lee BH. Assessment of bone mineral status in children with Marfan syndrome. American Journal of Medical Genetics Part A. 2012 Sep;158A(9):2221–4.
14. Hansen S, Shanbhogue V, Folkestad L, Nielsen MMF, Brixen K. Bone Microarchitecture and Estimated Strength in 499 Adult Danish Women and Men: A Cross-

Sectional, Population-Based High-Resolution Peripheral Quantitative Computed Tomographic Study on Peak Bone Structure. Calcified Tissue International. 2014 Mar;94(3):269–81.
15. Burghardt AJ, Buie HR, Laib A, Majumdar S, Boyd SK. Reproducibility of direct quantitative measures of cortical bone microarchitecture of the distal radius and tibia by HR-pQCT. Bone. 2010 Sep;47(3):519–28.
16. Nishiyama KK, Macdonald HM, Buie HR, Hanley DA, Boyd SK. Postmenopausal Women With Osteopenia Have Higher Cortical Porosity and Thinner Cortices at the Distal Radius and Tibia Than Women With Normal aBMD: An *In Vivo* HR-pQCT Study. Journal of Bone and Mineral Research. 2009 Oct 19;091019190442039–30.
17. Laib A, Hildebrand T, Häuselmann HJ, Rüegsegger P. Ridge number density: A new parameter for in vivo bone structure analysis. Bone. 1997 Dec;21(6):541–6.
18. Pistoia W, van Rietbergen B, Lochmüller E-M, Lill CA, Eckstein F, Rüegsegger P. Image-based micro-finite-element modeling for improved distal radius strength diagnosis: moving from bench to bedside. J Clin Densitom. 2004;7(2):153–60.
19. Hansen S, Beck Jensen J-E, Rasmussen L, Hauge EM, Brixen K. Effects on bone geometry, density, and microarchitecture in the distal radius but not the tibia in women with primary hyperparathyroidism: A case-control study using HR-pQCT. Journal of Bone and Mineral Research. 2010 Sep;25(9):1941–7.
20. Gordon CM, Zemel BS, Wren TAL, Leonard MB, Bachrach LK, Rauch F, Gilsanz V, Rosen CJ, Winer KK. The Determinants of Peak Bone Mass. The Journal of Pediatrics. 2017 Jan 1;180:261–9.
21. Bouxsein ML. Determinants of skeletal fragility. Best Practice & Research Clinical Rheumatology. 2005 Dec;19(6):897–911.
22. Mikolajewicz N, Bishop N, Burghardt AJ, Folkestad L, Hall A, Kozloff KM, Lukey PT, Molloy-Bland M, Morin SN, Offiah AC, Shapiro J, Rietbergen B, Wager K, Willie BM, Komarova SV, Glorieux FH. HR-pQCT Measures of Bone Microarchitecture Predict Fracture: Systematic Review and Meta-analysis. Journal of Bone and Mineral Research [Internet]. 2019 Oct 23 [cited 2019 Oct 28]; Available from: https://onlinelibrary.wiley.com/doi/abs/10.1002/jbmr.3901
23. Hansen S, Jensen J-EB, Ahrberg F, Hauge EM, Brixen K. The Combination of Structural Parameters and Areal Bone Mineral Density Improves Relation to Proximal Femur Strength: An In Vitro Study with High-Resolution Peripheral Quantitative Computed Tomography. Calcif Tissue Int. 2011 Aug 28;89(4):335.
24. Trifirò G, Mora S, Marelli S, Luzi L, Pini A. Increased fracture rate in children and adolescents with Marfan syndrome. Bone. 2020 Mar 25;115333.
25. Bouxsein ML. Bone quality: where do we go from here? Osteoporos Int. 2003 Sep 1;14(5):118–27.
26. Bouxsein ML, Karasik D. Bone geometry and skeletal fragility. Current Osteoporosis Reports. 2006 Jun;4(2):49–56.
27. Pereira L, Lee SY, Gayraud B, Andrikopoulos K, Shapiro SD, Bunton T, Biery NJ, Dietz HC, Sakai LY, Ramirez F. Pathogenetic sequence for aneurysm revealed in mice underexpressing fibrillin-1. Proc Natl Acad Sci U S A. 1999 Mar 30;96(7):3819–23.
28. Nistala H, Lee-Arteaga S, Carta L, Cook JR, Smaldone S, Siciliano G, Rifkin AN, Dietz HC, Rifkin DB, Ramirez F. Differential effects of alendronate and losartan therapy on

osteopenia and aortic aneurysm in mice with severe Marfan syndrome. Hum Mol Genet. 2010 Dec 15;19(24):4790–8.
29. Kanis JA, Cooper C, Rizzoli R, Reginster J-Y. European guidance for the diagnosis and management of osteoporosis in postmenopausal women. Osteoporosis International. 2019 Jan;30(1):3–44.
30. Seeman E. Structural basis of growth-related gain and age-related loss of bone strength. Rheumatology (Oxford). 2008 Jul;47(Suppl 4):iv2–8.
31. Zebaze RM, Ghasem-Zadeh A, Bohte A, Iuliano-Burns S, Mirams M, Price RI, Mackie EJ, Seeman E. Intracortical remodelling and porosity in the distal radius and post-mortem femurs of women: a cross-sectional study. The Lancet. 2010 May 15;375(9727):1729–36.
32. Zebaze RM, Libanati C, Austin M, Ghasem-Zadeh A, Hanley DA, Zanchetta JR, Thomas T, Boutroy S, Bogado CE, Bilezikian JP, Seeman E. Differing effects of denosumab and alendronate on cortical and trabecular bone. Bone. 2014 Feb 1;59:173–9.
33. Zebaze R, Libanati C, McClung MR, Zanchetta JR, Kendler DL, Høiseth A, Wang A, Ghasem-Zadeh A, Seeman E. Denosumab Reduces Cortical Porosity of the Proximal Femoral Shaft in Postmenopausal Women With Osteoporosis. Journal of Bone and Mineral Research. 2016;31(10):1827–34.
34. Folkestad L, Hald JD, Hansen S, Gram J, Langdahl B, Abrahamsen B, Brixen K. Bone geometry, density, and microarchitecture in the distal radius and tibia in adults with osteogenesis imperfecta type I assessed by high-resolution pQCT. J. Bone Miner. Res. 2012 Jun;27(6):1405–12.
35. Bonaretti S, Majumdar S, Lang TF, Khosla S, Burghardt AJ. The comparability of HR-pQCT bone measurements is improved by scanning anatomically standardized regions. Osteoporos Int. 2017 Jul;28(7):2115–28.
36. Shanbhogue VV, Hansen S, Halekoh U, Brixen K. Use of Relative vs Fixed Offset Distance to Define Region of Interest at the Distal Radius and Tibia in High-Resolution Peripheral Quantitative Computed Tomography. Journal of Clinical Densitometry. 2015 Apr 1;18(2):217–25.
37. Loeys BL, Dietz HC, Braverman AC, Callewaert BL, De Backer J, Devereux RB, Hilhorst-Hofstee Y, Jondeau G, Faivre L, Milewicz DM, Pyeritz RE, Sponseller PD, Wordsworth P, De Paepe AM. The revised Ghent nosology for the Marfan syndrome. Journal of Medical Genetics. 2010 Jul 1;47(7):476–85.

Figure Legends

Figure 1 Areal total spine and total hip bone mineral density in Marfan syndrome and controls

Legend: The figure show the areal BMD to the total spine and total hip. Each point indicate individual values of aBMD. The box represent the group median and inter quartile range. Solid points indicate the Marfan syndrome group, circles indicate the reference group. Both total spine and total hip aBMD is significantly lower in the Marfan syndrome group. Circles indicate women participants, squares indicate male participants.

Figure 2 Microarcitechtural features in Marfan syndrome and controls in the radius

Legend: The graph shows the estimated failure load, cortical porosity, trabecular number, trabecular area and volumetric bone mineral density in the radius comparing patients with Marfan syndrome (MFS) to the reference group (ref.gr) as assessed by HR-pQCT. The data is plotted against age for the two groups to visualize changes over time, as indicated by the fitted lines. Each parameter is chosen as the parameter that best differentiated between the Marfan syndrome group and the reference group. N= Newton, mm=millimeters, mgHA=milligram hydroxyapatite, vBMD= volumetric bone mineral density.

Figure 3 Microarcitechtural features in Marfan syndrome and controls in the tibia

Legend: The graph shows the estimated failure load, cortical porosity, trabecular number, trabecular area and volumetric bone mineral density in the radius comparing patients with Marfan syndrome (MFS) to the reference group (ref.gr) as assessed by HR-pQCT. The data is plotted against age for

the two groups to visualize changes over time, as indicated by the fitted lines. Each parameter is chosen as the parameter that best differentiated between the Marfan syndrome group and the reference group. N= Newton, mm=millimeters, mgHA=milligram hydroxyapatite, vBMD= volumetric bone mineral density.

Tables:

Table 1 - Participant characteristics

	Patients with MFS	Reference group	p-value
Participants (N)	74	146	NA
Median age [IQR]	40 [30-53]	37 [27-47]	0.45
Men (n (%))	32 (43%)	64 (44%)	NA
Women (n (%))	42 (57%)	82 (56%)	NA
Postmenopausal women (n (%))	13 (32%)	22 (27%)	0.28
Height (median cm [IQR])	184 [177-193]	172 [167-179]	<0.001
Weight (median kg [IQR])	81.1 [68.3-93.2]	76.2 [66.3-85.3]	0.09
BMI (kg/m^2)	22.8 [21.3-26.4]	25.3 [23.0-28.4]	0.002
DXA hip (n (%))	72 (97%)	144 (99%)	NA
DXA spine (n (%))	70 (95%)	145 (100%)	NA
HR-pQCT (n (%)), radius	63 (85%)	142 (98%)	NA
HR-pQCT (n (%)), tibia	74 (100%)	140 (97%)	NA

Legend: The table shows the participant characteristics. IQR = Inter Quartile Range NA = Not Applicable

Table 2 – High Resolution Peripheral Quantitative Computed Tomography parameters, radius

	Patients with MFS	Reference individuals	p-value	AIC	GOF
Geometry (mm^2)					
Total area	378 [322-438]	270 [231-336]	<0.0001	207.5	189
Cortical area	58±13	67±15	<0.0001	237.7	156
Trabecular area	324 [276-375]	204 [167-271]	<0.0001	197.0	184
Volumetric density (mgHA/cm3)					
Total vBMD	258±56	364±72	<0.0001	164.1	172
Cortical vBMD	849 [815-897]	928 [887-970]	<0.0001	188.6	173
Trabecular vBMD	149.0±36.5	184.9±44.0	<0.0001	224.5	177
Microarchitecture					
Trabecular number (1/mm)	1.80±0.30	1.98±0.28	<0.0001	235.6	109
Trabecular separation (mm)	0.51 [0.44-0.55]	0.42 [0.38-0.47]	<0.0001	235.8	209
Trabecular thickness (mm)	0.07±0.01	0.08±0.01	<0.001	237.7	198
Cortical thickness (mm)	0.76±0.18	1.02±0.20	<0.0001	186.2	207
Cortical porosity (%)	1.900 [1.200-2.600]	0.015 [0.010-0.023]	<0.0001	*	n.a
Bone strength (*N*)					
Failure load	4283 [3481-5001]	4497 [3724-5613]	0.09	249.7	204

Legends: The table shows the summery data regarding the HR-pQCT results for bone geometry, volumetric density and microarchitecture. vBMD = volumetric Bone Mineral Density shown in milligrams Hydroxy Apatite per cubic centimeter (gHA/cm^3). AIC = Akaike information criterion, GOF = Goodness-of-fit. The lower the AIC and the highest Goodness of fit indicates the variable that best distinguish between MFS and the reference group. * Cortical porosity predicts data perfectly

Table 3 - High Resolution Peripheral Quantitative Computed Tomography parameters, Tibia

Tibia	Patients with MFS	Reference individuals	p-value	AIC	GOF
Geometry ($mm^{2)}$					
Total area	985 [856-1174]	734 [660-847]	<0.0001	209.7	196
Cortical area	96 [77-116]	127 [112-147]	<0.0001	200.0	200
Trabecular area	901 [765-1068]	608 [535-708]	<0.0001	191.7	188
Volumetric density (mgHA/cm3)					
Total vBMD	223±48	322±58	<0.0001	154.7	174
Cortical vBMD	844 [808-869]	903 [867-932]	<0.0001	220.2	189
Trabecular vBMD	155±36	199±40	<0.0001	223.1	176
Microarchitecture					
Trabecular number (1/mm)	1.85±0.33	2.05±0.28	<0.0001	252.2	87
Trabecular separation (mm)	0.49 [0. 41-0.54]	0.41 [0.37-0.46]	<0.0001	241.3	214
Trabecular thickness (mm)	0.072 [0.063-0.080]	0.080 [0.071-0.091]	<0.0001	253.8	211
Cortical thickness (mm)	0.85±0.21	1.30±0.26	<0.0001	140.1	211
Cortical porosity (%)	4.850 [3.300-6.350]	0.049 [0.037-0.066]	<0.0001	*	n.a
Bone strength (*N*)					
Failure load	10909 [9441-12745]	11769 [10236-14195]	<0.05	271.1	213

Legends: The table shows the summery data regarding the HR-pQCT results for bone geometry, volumetric density and microarchitecture. vBMD = volumetric Bone Mineral Density shown in milligrams Hydroxy Apatite per cubic centimeter (gHA/cm^3). AIC = Akaike information criterion, GOF = Goodness-of-fit. The lower the AIC and the highest Goodness of fit indicates the variable that best distinguish between MFS and the reference group. * Cortical porosity predicts data perfectly

Table 4 – Circulating levels of Bone Turnover Markers and Sex Steroids in Marfan syndrome group and the reference individuals.

	MFS	Reference individuals	p-value
CTX (ng/L)	48 [33-0.65]	43 [31-68]	0.67
P1NP (μg/L)	72 [60-87]	51 [41-69]	<0.001
Male Participants			
FSH (IU/L)	4.85 [3.58-9.91]	4.38 [3.37-6.95]	0.32
LH (IU/L)	5.50 [3.34-7.99]	5.45 [3.67-6.38]	0.86
SHBG (nmol/l)	43.01[34.86-63.96]	39.55 [31.53-51.77]	0.32
17β-Estradiol	118.00 [85.1-135.0]	65.7 [55.25-77.75]	<0.0001
Testosterone (nmol/l)	15.7 [IQR 11.2-20.5]	15.7 [IQR 12.4-19.4]	0.88
Pre-menopausal women			
FSH (IU/L)	5.28 [3.72-7.07]	5.84 [3.73-8.93]	0.42
LH (IU/L)	5.87 [4.02-10.78]	6.99 [3.36-11.75]	0.61
SHBG (nmol/l)	94.82 [68.07-127.0]	79.84 [53.34-127.3]	0.46
17β-Estradiol (nmol/l)	215.5 [53.7-547]	202 [120-426]	0.98
Testosterone (nmol/l)	0.71 [0.57-1.01]	1.1 [0.78-1.7]	<0.0002
Post-menopausal women			
FSH (IU/L)	62.5 [43.4-79.0]	78.0 [37.2-97.2]	0.31
LH (IU/L)	35.1 [26.2-40.6]	37.4 [24.8-47.2]	0.93
SHBG (nmol/l)	61.2 [47.9-95.6]	64.5 [51.5-93.1]	0.96
17β-Estradiol (nmol/l)	32.4 [<15-83.7]	<15 [<15-35.4]	0.16
Testosterone (nmol/l)	0.66 [0.50-1.00]	0.94 [0.76-1.3]	0.06

Legends: The table shows the summery data regarding circulating levels bone turnover markers and sex hormones. CTX= carboxyterminal cross-linked telopeptide of type 1 collagen, P1NP = N-terminal propeptide of type 1 procollagen FSH = follicle stimulating hormone , LH = luteinizing hormone, SHBG =sex hormone binding globulin